Fermi resonance in optical microcavities

Chang-Hwan Yi, Hyeon-Hye Yu, and Ji-Won Lee
Department of Physics, Sogang University, Seoul 121-742, Korea

Chil-Min Kim*
Department of Emerging Materials Science, Daegu Gyeongbuk Institute of Science and Technology, Hyeonpung-myeon Dalseong-gun, Daegu 711-873, Korea

(Received 12 March 2014; published 8 April 2015)

Fermi resonance is a phenomenon of quantum mechanical superposition, which most often occurs between normal and overtone modes in molecular systems that are nearly coincident in energy. We find that scarred resonances in deformed dielectric microcavities are the very phenomenon of Fermi resonance, that is, a pair of quasinormal modes interact with each other due to coupling and a pair of resonances are generated through an avoided resonance crossing. Then the quantum number difference of a pair of quasinormal modes, which is a consequence of quantum mechanical superposition, equals periodic orbits, whereby the resonances are localized on the periodic orbits. We derive the relation between the quantum number difference and the periodic orbits and confirm it in an elliptic, a rectangular, and a stadium-shaped dielectric microcavity.

DOI: 10.1103/PhysRevE.91.042903 PACS number(s): 05.45.Mt, 42.55.Sa, 42.60.Da

I. INTRODUCTION

Eigenfunctions localized on unstable periodic orbits of classical dynamics [1,2] in a stadium-shaped billiard [3] were named scars by Heller [4]. Since then, scars were observed in various chaotic systems such as quantum dots, microwave, and atomic and molecular systems [5–10]. In deformed dielectric microcavities, scarred resonances, localized on periodic orbits, were also observed [11,12]. Even in nonchaotic systems such as an elliptic and a rectangular dielectric microcavity, nontrivial resonances, named scarlike resonances (SLRs), were found [13,14], which occur through an avoided resonance crossing (ARC) caused by the openness of the cavity. These SLRs were experimentally confirmed in an elliptic microcavity laser and were shown to be localized on the nonisolated periodic orbits [15].

It was also found that scars in a molecular system are the phenomenon of Fermi resonance [8]. The phenomenon was confirmed in a hydrogen atom in a magnetic field [7] and in several molecular systems [8–10]. In these systems, when two eigenstates are coupled, the Fermi resonance occurs through an avoided level crossing [7–10] and another pair of eigenstates are generated, which are scars. The transition is describable as a linear combination of a pair of parent modes, i.e., quantum mechanical superposition. In these systems, Fermi resonance is caused by coupling between two nearly degenerated eigenstates [7–9]. It was also shown that the scarred states in molecular systems are always generated due to broad avoided level crossing [16].

However, Fermi resonance has not been yet studied in dielectric microcavities despite it being a common phenomenon for the formation of scars in atomic and molecular systems. In this paper we show that SLRs and scarred resonances in dielectric microcavities are Fermi resonances and confirm it first in an elliptic and a rectangular dielectric microcavity as integrable systems and then in a stadium-shaped dielectric microcavity as a chaotic system. Through the study, we find that a pair of SLRs or a pair of scarred resonances is caused by the interaction between a pair of quasinormal modes through an ARC, whereby the scarred resonances are localized on unstable periodic orbits, while SLRs are localized on nonisolated periodic orbits.

This paper is organized as follows. In Sec. II we derive the Fermi resonance relation in a two-dimensional microcavity. In Sec. III we demonstrate Fermi resonance in an elliptic microcavity. In Sec. IV we demonstrate Fermi resonance in a rectangular and a stadium-shaped microcavity. We discuss the phenomenon of Fermi resonance in several microcavities and summarize our results in Sec. IV.

II. FERMI RESONANCE RELATION

In dielectric microcavities, the nonzero off-diagonal terms in a Hamiltonian for an ARC [13] are the coupling between two nearly degenerated quasinormal modes for Fermi resonance. Then we can obtain the relation between the quantum number difference of a pair of quasinormal modes, i.e., quantum mechanical superposition, and the periodic orbits supporting scarred resonances in two-dimensional optical microcavities. In these cavities, the Hamiltonians of two quasinormal modes can be described by $H(I_1,I_2)$ and $H(I_1',I_2')$, where I_i and I_i' are the action variables and the subscripts 1 and 2 are the degrees of freedom. Because $|I_i' - I_i| \ll 1$ in nearly degenerated states, we can obtain the following condition by expanding $H(I_1',I_2')$:

$$(I_1 - I_1')\omega_1 + (I_2 - I_2')\omega_2 = 0, \tag{1}$$

where $\omega_i = \partial H/\partial I_i$ is the frequency associated with the action I_i. Since $I_i = (n_i + \alpha_i/4)$, we can obtain the relation $|n_1 - n_1'|\omega_1 = |n_2 - n_2'|\omega_2$ for two eigenstates (n_1,n_2) and (n_1',n_2'), where α_i is the Maslov index. According to Berry and Tabor, when the winding number ω_1/ω_2 is rational, the orbit is periodic [17]. Then we can obtain the following relation for Fermi resonance:

$$(|\Delta n_1|,|\Delta n_2|) = (m_2,m_1), \tag{2}$$

*chmkim@dgist.ac.kr

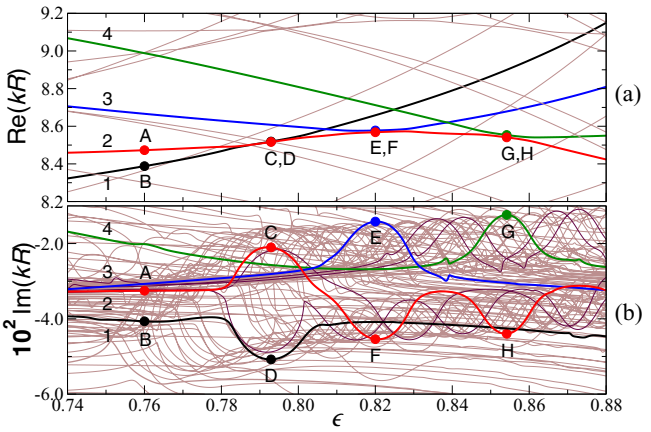

FIG. 1. (Color online) Eigenvalues in an elliptic microcavity depending on the eccentricity: (a) the real eigenvalues and (b) the imaginary eigenvalues. Curves 1, 2, 3, and 4 exhibit resonance trapping for bow-tie SLRs and their pairs through ARCs.

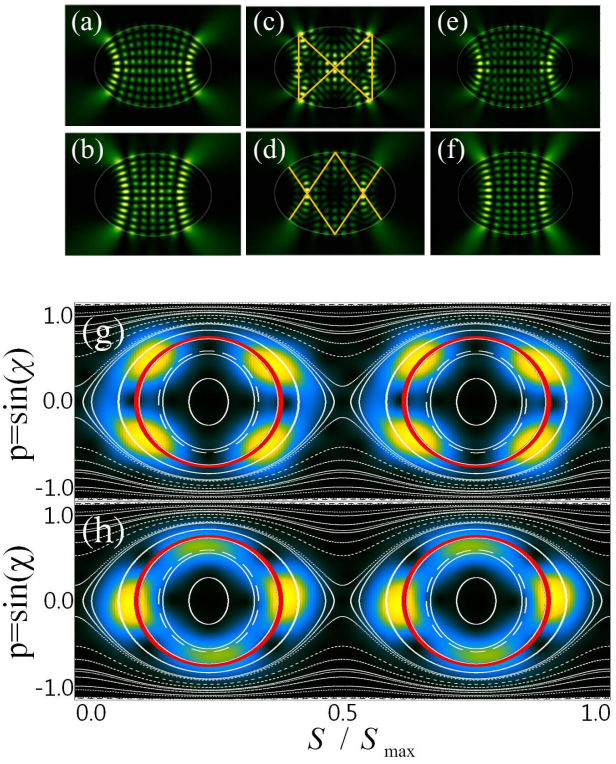

FIG. 2. (Color online) Intensity plots and Husimi functions of resonances in an elliptic microcavity depending on ϵ. (a) and (b) Bouncing-ball-type quasinormal modes before an ARC at $\epsilon = 0.76$. (c) and (d) Bow-tie SLR and its pair, respectively, at $\epsilon = 0.793$. (e) and (f) Recovered bouncing-ball-type resonances after the ARC at $\epsilon = 0.81$. (g) and (h) Husimi functions of (c) and (d), respectively. In the Husimi functions, thick solid elliptic lines are resonant tori corresponding to the (4,1) periodic orbit. Here χ is the incident angle, S is the arc length from the x axis, and S_{max} is the total boundary length.

where (m_2,m_1) is the classical periodic orbit, which should be determined according to the cavity morphology, and $(|\Delta n_1|,|\Delta n_2|)$ is the quantum number difference of two quantum states (n_1,n_2) and (n_1',n_2'). Here $|\Delta n_1| = |n_1 - n_1'|$ and $|\Delta n_2| = |n_2 - n_2'|$ are the quantum number differences on each degree of freedom and m_1 and m_2 are the integer numbers associated with frequencies ω_1 and ω_2, respectively, which indicates the repeating numbers on each degree of freedom for a periodic orbit. Because the Fermi resonance relation indicates that the quantum number difference equals the periodic orbit, the quantum state $(|\Delta n_1|,|\Delta n_2|)$, which is the superposed state of parent quasinormal modes, should be localized on the periodic orbit (m_2,m_1). Then the superposed state is a scarred resonance or an SLR and this is the phenomenon of Fermi resonance in dielectric microcavities.

III. FERMI RESONANCE IN AN ELLIPTIC MICROCAVITY

For a deeper understanding of Fermi resonance, first we focus on bow-tie SLRs and their pairs in an elliptic dielectric microcavity. The region of the nonisolated bow-tie orbits supporting the bow-tie SLRs and their pairs is about $\epsilon > 0.71$ [18–21]. Here ϵ is the eccentricity given by $\epsilon = \sqrt{1-(b/a)^2}$, where a and b are the major and the minor radius of the ellipse, respectively. When the transverse-magnetic (TM) polarized resonances are obtained in the region $kR < 15$ and $\epsilon < 0.95$ depending on ϵ by preserving the cavity area, complicated ARCs occur, where k is the vacuum wave number and $R = \sqrt{ab}$.

Figures 1(a) and 1(b) are the real and the imaginary eigenvalue of even-odd modes in the region $0.74 < \epsilon < 0.88$, respectively, which are obtained by solving the Helmholtz equation by the boundary element method [22] for the effective refractive index of 3.3. Among the curves we choose four arbitrary ones, whose parent modes are bouncing-ball-type quasinormal modes. Curve 2 is of interest, which interacts with the others three times. Curve 2 starting at point A interacts with curve 1 around $\epsilon = 0.793$ by level crossing. Next it interacts with curve 3 around $\epsilon = 0.820$ and with curve 4 around $\epsilon = 0.854$ by level repulsion. Several more curves (thick violet) are presented to show similar multiple interactions. When ARCs take place, the distance between the imaginary eigenvalues of the pairs is maximized, which is resonance trapping appearing in open systems [23–25]. When interaction occurs, the quasinormal modes transit to a bow-tie SLR and its pair of SLRs.

In order to show ARCs for the bow-tie SLRs and their pairs, we obtain the intensity plots and Husimi functions of the resonances around $\epsilon = 0.793$. The resonances in Figs. 2(a) and 2(b) are bouncing-ball-type quasinormal modes at points A and B, respectively. When an ARC takes place due to interaction of curves 1 and 2, a bow-tie SLR and its pair are generated as shown in Figs. 2(c) and 2(d), respectively. Figure 2(c) shows a bow-tie SLR at point C and Fig. 2(d) its pair at point D, which is of a superposed shape of V and Λ, as shown by the trajectories superimposed on the wave functions. The pair of SLRs belongs to the same SLR family, which is localized on the nonisolated periodic orbits [15]. After the ARC, the parent modes of the bouncing-ball-type quasinormal modes are recovered around $\epsilon = 0.81$ without exchanging their patterns due to a weak ARC as shown in Figs. 2(e) and 2(f), respectively. Similarly, the resonances at points E and G

in Fig. 1 are bow-tie SLRs and those at points F and H in Fig. 1 are their pairs. After the ARCs, their parent modes are recovered with exchanging their patterns due to a strong ARC. As the two bouncing-ball-type quasinormal modes interact with each other, a recovered quasinormal mode interacts again with another one for another pair of SLRs. Hence multiple interactions take place for the bow-tie SLRs and their pairs.

In order to show the localization of the SLRs in Figs. 2(c) and 2(d) on the bow-tie SLR and its pair of periodic orbits, the Husimi functions superimposed on the classical trajectories are obtained as shown in Figs. 2(g) and 2(h), respectively. The thick solid ellipsis (red) in each figure is the (4,1) resonant torus. Each figure clearly shows that the four bright spots are localized on the (4,1) resonant torus and that the positions of the bright spots in Figs. 2(g) and 2(h) coincide with the trajectory shown in Figs. 2(c) and 2(d), respectively. Hence, the four bright spots of each Husimi function are evidence of the localization on each nonisolated periodic orbit.

Because Fermi resonance is a quantum mechanical superposition defined by a quantum number difference, we obtain the quantum number difference of a pair of bouncing-ball-type quasinormal modes. When the degrees of freedom denoted by the subscripts 1 and 2 are replaced with e and h, which are the elliptic and the hyperbolic axis in the elliptic coordinate, the quantum numbers of the quasinormal modes in Figs. 2(a) and 2(b) are $(n_e,n_h) = (11,5)$ and (7,6), respectively, where n_e and n_h are the elliptic and the hyperbolic quantum number, respectively. Then the quantum number difference is $(|\Delta n_e|,|\Delta n_h|) = (4,1)$, which is the Fermi resonance. Similarly, the (15,4) and (11,5) quasinormal modes interact with each other around $\epsilon = 0.854$ and a bow-tie SLR and its pair, whose quantum number difference is $(|\Delta n_e|,|\Delta n_h|) = (4,1)$, are generated. Also the (19,3) and (15,4) quasinormal modes interact with each other and a bow-tie SLR and its pair are generated. According to the relation in Eq. (2), the bow-tie SLRs and their pairs should be localized on the $(m_h,m_e) = (4,1)$ periodic orbits. In an elliptic cavity, because m_h and m_e are the number of reflections of an orbit on the boundary and its libration number between two hyperbolic caustics [18], respectively, the periodic orbit is $(m_h,m_e) = (4,1)$, whereby the bow-tie SLR and its pair of SLRs are localized on the periodic orbits. The period of the nonisolated periodic orbit in Figs. 2(g) and 2(h), where the bow-tie SLR and its pair of SLRs are localized, is $(m_h,m_e) = (4,1)$. In our further investigation, all the pairs of bow-tie SLRs in an elliptic cavity satisfy the relation $(|\Delta n_e|,|\Delta n_h|) = (m_h,m_e) = (4,1)$.

Other evidence of Fermi resonance is the quantum mechanical superposition of parent quasinormal modes. To show it, a pair of bouncing-ball-type quasinormal modes of $(n_e,n_h) = (11,5)$ and (7,6) are superposed. As shown in Figs. 3(a) and 3(b), the superposed states $[(11,5) + (7,6)]/\sqrt{2}$ and $[(11,5) - (7,6)]/\sqrt{2}$ are a bow-tie SLR and its pair, whose patterns are the same as those in Figs. 2(c) and 2(d), respectively. This result indicates that SLRs localized on nonisolated periodic orbits are caused by Fermi resonance.

The generation of a bow-tie SLR and its pair of SLRs is of high interest because they are localized on the same resonant torus. According to the Birkhoff-Poincaré theorem, when a resonant torus is destroyed, a stable and an unstable periodic orbit are generated as a pair. In a soft chaotic system, when an ARC takes place, a pair of eigenfunctions is localized on the pair of periodic orbits. An eigenfunction localized on the unstable periodic orbit is a scar and its pair is localized on the stable periodic orbit. This phenomenon was demonstrated in the Harper map [26]. In our case, because a resonant torus is not destroyed, the generation of a pair of SLRs cannot be explained in such terms. However, because the trajectories of a pair of SLRs are on the same resonant torus, we can say that they are a pair. This phenomenon is caused by the openness of the system [13].

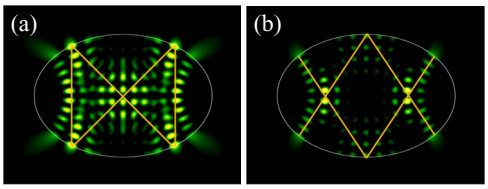

FIG. 3. (Color online) Intensity plots of superposed resonances: (a) the addition of two bouncing-ball-type quasinormal modes $[(11,5) + (7,6)]/\sqrt{2}$ whose shape is a bow tie and (b) the subtraction $[(11,5) - (7,6)]/\sqrt{2}$.

IV. FERMI RESONANCE IN OTHER MICROCAVITIES

We also confirm Fermi resonance in a rectangular dielectric microcavity for the effective refractive index of 3.3. When a square microcavity deforms to a rectangular one, we obtain the real and imaginary eigenvalues of even-odd modes in the region $0.0 < \epsilon = 1 - b/a < 0.16$ and $9.0 < k < 9.6$ by preserving the cavity area, where k is the vacuum wave number and a and b are the horizontal and the vertical cavity length, respectively. The eigenvalues and resonances are obtained by solving the Helmholtz equation by the boundary element method [22].

Figures 4(a) and 4(b) are the real and imaginary eigenvalues, respectively, which also show complicated interactions among the resonances. Of these, we choose four arbitrary curves from 1–4, whose parent modes are the $(n_x,n_y) = (6,3)$, (14,5), (10,11), and (12,9) quasinormal modes, respectively,

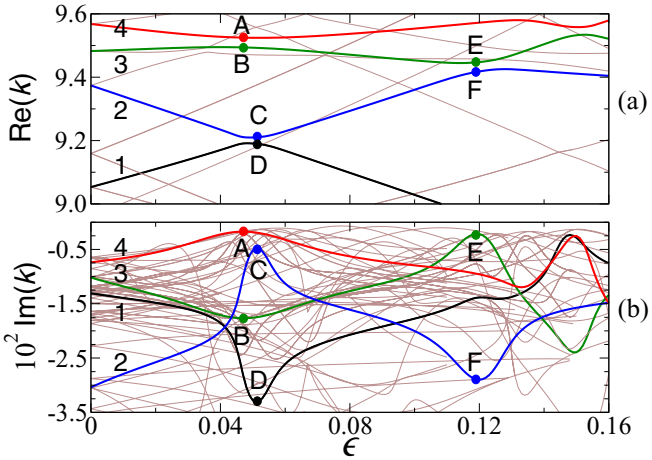

FIG. 4. (Color online) Eigenvalues in a rectangular microcavity depending on the deformation parameter ϵ: (a) the real eigenvalues and (b) the imaginary eigenvalues.

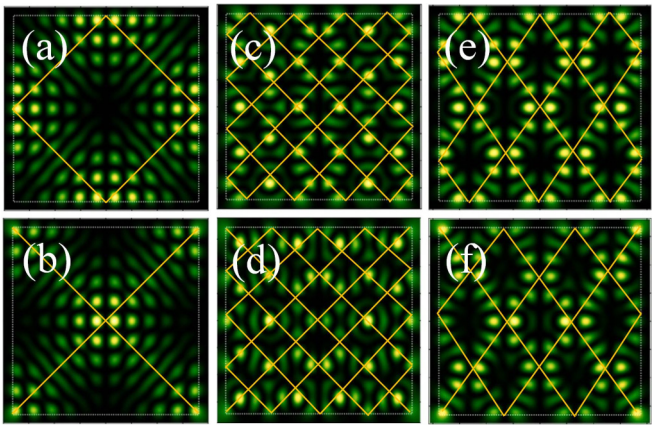

FIG. 5. (Color online) Pairs of SLRs in a rectangular dielectric microcavity at (a) and (b) points A and B, respectively, around $\epsilon = 0.046$; (c) and (d) points C and D, respectively, around $\epsilon = 0.051$; and (e) and (f) points E and F, respectively, around $\epsilon = 0.119$ in Fig. 4. The lines are the trajectories of the nonisolated periodic orbits where the SLRs are localized.

where x and y are the orthogonal axes in Cartesian coordinates. Curves 1 and 2 interact with each other around $\epsilon = 0.051$, curves 3 and 4 around $\epsilon = 0.046$, and curves 2 and 3 around $\epsilon = 0.119$. The imaginary eigenvalues indicate that the interactions are resonance trapping. In each interaction, a pair of parent quasinormal modes is recovered after ARCs by exchanging their property for the next ARCs. During the interactions SLRs are generated, satisfying the Fermi resonance relation.

Three pairs of TM polarized resonances are taken as examples as shown in Fig. 5. Figures 5(a) and 5(b) are the SLRs at $\epsilon = 0.046$, where curves 3 and 4 interact with each other. Because the SLRs are localized on a diamond-shaped and an X-shaped orbit, respectively, the trajectories superimposed on the resonances bounce twice for a single round-trip. Since the (m_y,m_x) periodic orbit is defined by the total bouncing number on each axis, the nonisolated periodic orbit is $(m_y,m_x) = (2,2)$. Because the SLRs are the result of the interaction between the (10,11) and (12,9) quasinormal modes, the quantum number difference is $(|\Delta n_x|,|\Delta n_y|) = (2,2)$. Hence the SLRs satisfy the Fermi resonance relation such that $(|\Delta n_x|,|\Delta n_y|) = (m_y,m_x) = (2,2)$. Similarly, since the SLRs shown in Figs. 5(c) and 5(d) are caused by the interaction between the (6,13) and (14,5) quasinormal modes around $\epsilon = 0.051$, the quantum number difference of the SLRs is $(|\Delta n_x|,|\Delta n_y|) = (8,8)$, which equals the nonisolated periodic orbit $(m_y,m_x) = (8,8)$ as the trajectories are shown in the figures. Also, the SLRs shown in Figs. 5(e) and 5(f) are caused by the interaction between the (6,13) and (12,9) quasinormal modes at $\epsilon = 0.119$. The SLRs satisfy the relation $(|\Delta n_x|,|\Delta n_y|) = (m_y,m_x) = (6,4)$.

As an example of Fermi resonance in chaotic dielectric microcavities, we take a stadium-shaped one. As the deformation parameter $\epsilon = L/R$ increases, the real and imaginary eigenvalues of transverse electric polarized resonances are obtained for a refractive index of 3.3, where L is the linear section length and R the radius of a circle. Among the resonances we focus on the interaction of the $(n_r,n_\theta) = (2,m)$ and $(3,m-4)$ quasinormal modes for the quantum number difference $(|\Delta n_r|,|\Delta n_\theta|) = (1,4)$, where n_r and n_θ are the radial and the angular quantum number in a circular cavity, respectively. Figures 6(a) and 6(b) are the real and imaginary eigenvalues of the (2,36) and (3,32) quasinormal modes depending on ϵ. Both the real and imaginary eigenvalues exhibit a level repulsion, which is one of the ARCs in open systems. The figure shows that while the two real eigenvalues interact at the beginning of deformation, the two imaginary ones interact around $\epsilon = 0.01$. When we obtain resonances, they transit to scarred resonances when $\epsilon = 0.001$.

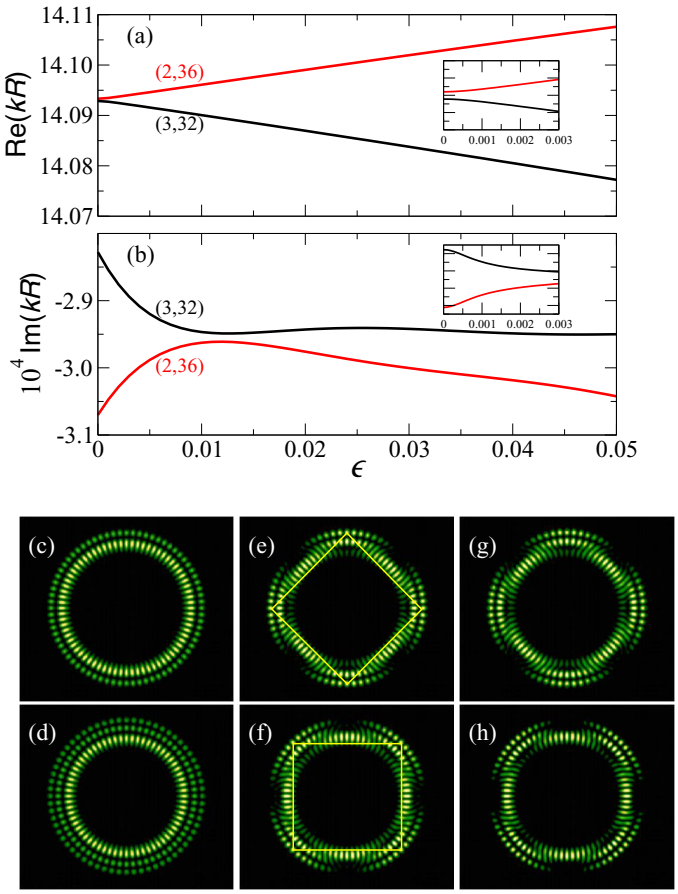

FIG. 6. (Color online) Eigenvalues and the resonances in a stadium-shaped microcavity depending on ϵ. (a) and (b) Real and imaginary eigenvalues of the (2,36) and (3,32) quasinormal modes. (c) and (d) The (2,36) and (3,32) quasinormal modes at $\epsilon = 0.0$, respectively. (e) and (f) The diamond-shaped scarred resonance and its pair of rectangular-shaped resonances at $\epsilon = 0.01$, respectively. (g) and (h) Superposed states of $[(2,36) - (3,32)]/\sqrt{2}$ and $[(2,36) + (3,32)]/\sqrt{2}$, respectively. The insets in (a) and (b) are the eigenvalues in the region of small deformation.

The intensity plots of the (2,36) and (3,32) quasinormal modes at $\epsilon = 0.0$ are shown in Figs. 6(c) and 6(d), respectively. When the two quasinormal modes interact with each other, a diamond-shaped and a rectangular scarred resonance are generated as shown in Figs. 6(e) and 6(f), respectively. The resonances are localized on the unstable period-4 orbits, which are $(m_\theta,m_r) = (1,4)$ as shown by the orbits superimposed on the resonances. Here m_θ and m_r are the number of rotations of the orbit around the center and its reflection number on

the boundary, respectively. The trajectory, when it travels one revolution on the angular axis, bounces four times on the radial axis. Hence the scarred resonances satisfy the periodic orbit $(m_\theta,m_r) = (1,4)$. In the figures we can see a slight mismatch between the orbit and the resonances, which is caused by an optical property of the Goos-Hänchen shift in a dielectric microcavity [27]. In the resonances, we can see two outer circles where the probability density is low. We attribute this phenomenon to interference. In our further investigation, when each pair of (l,m) and $(l+1,m-4)$ quasinormal modes interact with each other, scarred resonances of the similar patterns are generated.

In this cavity, the original quasinormal modes are not recovered after an ARC because of the destruction of invariant curves supporting the quasinormal modes. In order to show that the scarred resonances are the result of Fermi resonance, we obtain the superposed states of $[(2,36)-(3,32)]/\sqrt{2}$ and $[(2,36)+(3,32)]/\sqrt{2}$ as shown in Figs. 6(g) and 6(h), respectively. As shown in the figures, the superposed states are the same as the scarred resonances, which are of a diamond-shaped and a rectangular pattern, respectively.

In dielectric microcavities, when the quasinormal modes of a pair interact with each other through an ARC, Fermi resonance occurs. The off-diagonal terms in a Hamiltonian for an ARC are the coupling for Fermi resonance. Then we can sum up the conditions for Fermi resonance in dielectric microcavities as follows. (i) Two real eigenvalues should approach each other to become nearly degenerated states for interaction. (ii) The quantum number difference of the nearly degenerated quasinormal modes should equal a classical periodic orbit, where SLRs or scarred resonances are localized. Under these conditions Fermi resonance occurs for SLRs and scarred resonances through the interaction between two quasinormal modes. In our further investigation, we also find that scars in chaotic billiards are also the phenomenon of Fermi resonance.

V. DISCUSSION AND CONCLUSION

We have investigated Fermi resonance in dielectric microcavities of three shapes. Through the investigation, we found that the Fermi resonance relation coincides with the SLRs and scarred resonances. However, we emphasize that the conditions we have discussed cannot be directly applied to all systems. For example, first, in the case of nonchaotic billiards such as an elliptic and a rectangular one, although the eigenvalues of two eigenfunctions are coincident and there are various nonisolated periodic orbits, there is no Fermi resonance because the eigenfunctions do not interact with each other. Next, in a fully chaotic system, two nearly degenerated scarred resonances interact with each other and another pair of scarred resonances is generated. In this case, because scarred resonances have no well-defined quantum number, the quantum number difference is hard to determine for Fermi resonance [8]. Finally, it was shown that a quasiscarred resonance is a linear combination of a number of quasinormal modes with proper weighting factors [28,29], whose quantum number differences are $(|\Delta n_r|,|\Delta n_\theta|) = (1,3)$ and (2,5) for a triangular and a star shape, respectively, and that the orbits supporting the resonances exist due to uncertainty [30,31]. Although in this case the relation $(|\Delta n_\theta|,|\Delta n_r|) = (m_r,m_\theta)$ is satisfied, these resonances are not pairs of quasinormal modes. More rigorous studies are required for these exceptional cases.

In conclusion, we have verified that SLRs and scarred resonances are phenomena of Fermi resonance due to interaction between a pair of quasinormal modes through an ARC and why SLRs and scarred resonances are localized on periodic orbits. Our results provide a meaningful contribution to the understanding of scars and scarred resonances in chaotic microcavities.

ACKNOWLEDGMENTS

This research was supported by Basic Science Research Program (Grant No. NRF-2013R1A1A2060846) and High-Tech Convergence Technology Development Program (Grant No. NRF-2014M3C1A3051331) through the National Research Foundation of Korea (NRF) funded by the Ministry of Science, ICT & Future Planning.

[1] M. C. Gutzwiller, Phys. Rev. Lett. **45**, 150 (1980).
[2] G. Tanner, P. Scherer, E. B. Bogomonly, B. Eckhardt, and D. Wintgen, Phys. Rev. Lett. **67**, 2410 (1991).
[3] S. W. McDonald and A. N. Kaufman, Phys. Rev. Lett. **42**, 1189 (1979).
[4] E. J. Heller, Phys. Rev. Lett. **53**, 1515 (1984).
[5] *Optical Process in Microcavities*, edited by R. K. Chang and A. J. Campillo (World Scientific, Singapore, 1996).
[6] H. J. Stöckmann, *Quantum Chaos: An Introduction* (Cambridge University Press, Cambridge, 2000).
[7] J. R. Walkup, M. Dunn, D. K. Watson, and T. C. Germann, Phys. Rev. A **58**, 4668 (1998).
[8] F. J. Arranz, F. Borondo, and R. M. Benito, Phys. Rev. Lett. **80**, 944 (1998).
[9] B. Ramachandran and K. G. Kay, J. Chem. Phys. **99**, 3659 (1993).
[10] F. L. Robert and C. Jaffé, J. Chem. Phys. **99**, 2495 (1993).
[11] J. U. Nöckel and A. D. Stone, Nature (London) **385**, 45 (1997).
[12] C. Gmachl, F. Capasso, E. E. Narimanov, J. U. Nöckel, A. D. Stone, J. Faist, D. L. Sivco, and A. Y. Cho, Science **280**, 1556 (1998).
[13] J. Wiersig, Phys. Rev. Lett. **97**, 253901 (2006).
[14] J. Unterhinninghofen, J. Wiersig, and M. Hentschel, Phys. Rev. E **78**, 016201 (2008).
[15] C. H. Yi, S. H. Lee, M. W. Kim, J. Cho, J. Lee, S. Y. Lee, J. Wiersig, and C. M. Kim, Phys. Rev. A **84**, 041803(R) (2011).
[16] F. J. Arranz, L. Seidel, C. G. Giralda, R. M. Benito, and F. Borondo, Phys. Rev. E **82**, 026201 (2010).

[17] M. V. Berry and M. Tabor, Proc. R. Soc. London Ser. A **349**, 101 (1976).
[18] M. Sieber, J. Phys. A: Math. Gen. **30**, 4563 (1997).
[19] M. A. Bandres and J. C. Gutiérrez-Vega, Am. J. Phys. **72**, 810 (2004).
[20] A. G. Magner *et al.*, Prog. Theor. Phys. **102**, 551 (1999).
[21] H. Waalkens, J. Wiersig, and H. R. Dullin, Anal. Phys. **260**, 50 (1997).
[22] J. Wiersig, J. Opt. A **5**, 53 (2003).
[23] E. Persson, T. Gorin, and I. Rotter, Phys. Rev. E **58**, 1334 (1998).
[24] E. Persson, I. Rotter, H.-J. Stockmann, and M. Barth, Phys. Rev. Lett. **85**, 2478 (2000).
[25] Q. H. Song and H. Cao, Phys. Rev. Lett. **105**, 053902 (2010).
[26] D. A. Wisniacki, M. Saraceno, F. J. Arranz, R. M. Benito, and F. Borondo, Phys. Rev. E **84**, 026206 (2011).
[27] H. Schomerus and M. Hentschel, Phys. Rev. Lett. **96**, 243903 (2006).
[28] J. Lee, S. Rim, J. Cho, and C. M. Kim, Phys. Rev. Lett. **101**, 064101 (2008).
[29] C. C. Liu, T. H. Lu, Y. F. Chen, and K. F. Huang, Phys. Rev. E **74**, 046214 (2006).
[30] S. Y. Lee, S. Rim, J.-W. Ryu, T.-Y. Kwon, M. Choi, and C.-M. Kim, Phys. Rev. Lett. **93**, 164102 (2004).
[31] S.-Y. Lee, S. Rim, J.-W. Ryu, T.-Y. Kwon, M. Choi, and C.-M. Kim, J. Phys. A: Math. Theor. **41**, 275102 (2008).